

# Using Electrochemistry - Total Internal Reflection Ellipsometry Technique to Observe the Dissolved Oxygen Reduction on Clark Electrode



Wei Liu<sup>a,b</sup>, Meng Li<sup>a,b</sup>, Ziren Luo<sup>a</sup>, Gang Jin<sup>a,\*</sup>

<sup>a</sup> NML, Institute of Mechanics, Chinese Academy of Sciences, # 15, Bei-si-huan West Road, Beijing, 100190, China

<sup>b</sup> University of Chinese Academy of Sciences, # 19, Yu-quan Road, Beijing, 100049, China

## ARTICLE INFO

### Article history:

Received 29 April 2014

Received in revised form 18 July 2014

Accepted 21 July 2014

Available online 7 August 2014

### Keywords:

Total internal reflection ellipsometry

Clark electrode

Evanescence wave

Electrochemistry

Dissolved oxygen detection

## ABSTRACT

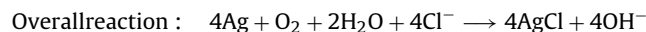
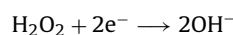
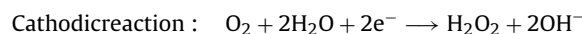
The high interface sensitivity in the ellipsometric phase shift,  $\Delta$ , makes total internal reflection ellipsometry (TIRE) a useful tool to study redox reactions on the electrode surface. Electrochemistry - total internal reflection ellipsometry (EC-TIRE) is proposed to observe the refractive index change induced by the reduction of the dissolved oxygen (DO) on Clark electrode. In order to analyze the TIRE signal change caused by the reaction, we have calculated the refractive index variation on the surface of Clark electrode. We have found that the calculation under the thin layer boundary condition is more persuasive than that under the semi-infinite boundary condition not only in the steady state measurement but in the dynamic process.

© 2014 Elsevier Ltd. All rights reserved.

## 1. Introduction

Total internal reflection ellipsometry (TIRE) technique has been proved as a powerful tool to study the corrosion of thin copper films [1], the adsorption and removal of substances from milk on metal surfaces [2] and the protein monolayers on thin gold films [3], for it is highly sensitive to various physics, chemical and biochemical processes on a substrate surface. The high interface sensitivity of TIRE arises from the fact that its detection is based on evanescent wave. Under total internal reflection condition, an evanescent wave would occur at the interface when light propagates from a dense medium to a rare one. Although the intensity of the evanescent wave at the interface can be amplified, larger than that of the input beam, it decays exponentially with the distance less than the wavelength from the interface [4]. By optimizing the incident angle, the polarization of the light beam and the thickness of the introduced thin gold layer [5], we use TIRE as the biosensor to detect cluster of differentiation 146 (CD146), a cell adhesion molecule used as a marker for endothelial cell lineage, quantitatively [6]. Despite many successful applications, it is seldom reported to use TIRE to monitor electrochemical reactions.

The measurement of DO is of great importance in industrial [7], medical [8] and environmental applications [9]. Clark electrode is a membrane-covered polarographic DO probe. When we polarize the electrode with a potential of  $-800$  mV (vs. Ag/AgCl), DO is reduced on the gold surface as follows [10]:



Because of the reduction, the reaction produces alkalinity in the medium with a small amount of hydrogen peroxide [11].

In general, Clark electrode works under a steady state condition when the current reduced from DO approaches stable. However, examples require relatively fast concentration change measurement [12–14]. The dynamic measurement of Clark electrode has been proposed, which measures the transient response of the electrode during the response time.

In this paper, we have demonstrated that the interface sensitivity in the ellipsometric phase shift,  $\Delta$ , makes TIRE an alternative to study electrochemical reactions in which neither reactants nor

\* Corresponding author. Fax: +86 1082544138.  
E-mail address: [gajin@imech.ac.cn](mailto:gajin@imech.ac.cn) (G. Jin).

products bind to the surface of the electrode. Then, we use EC-TIRE to study DO reduction on Clark electrode. To analyze the TIRE signal change caused by the reaction-induced index variation of refraction, a thin layer model under finite boundary condition is developed not only in the steady state measurement but in the dynamic measurement. The results have extended a new trial of TIRE technique.

## 2. Methodology and Experimental

### 2.1. EC-TIRE Principle and Operation

For the electrochemical reactions in which neither reactant- nor product- binding happens on the electrode surface, S. Wang, X. Huang, X. Shan, K. J. Foley and N. Tao have proposed that the SPR response by the reaction-induced refractive index change near the electrode can be given by [15]

$$\theta(t) = B \int_0^{\infty} [\alpha_O C_O(x, t) + \alpha_R C_R(x, t)] \exp(-x/l) d(x/l) \quad (1)$$

where  $C_O$  and  $C_R$  are the reactant and product concentrations,  $\alpha_O$  and  $\alpha_R$ , the local complex refractive index changes per unit concentration for the oxidized and reduced molecules, respectively.  $B$  is the sensitivity constant for a given SPR and reaction. The decay of evanescent wave from the metal into the solution phase is described by the exponential term in the integral and the decay length  $l$ , is around 100 nm. Although, in principle,  $l$  is also a function of  $C_O$  and  $C_R$ , a first order of approximation makes  $l$  a constant.

Eq (1) can be used to describe the local complex index of refraction:

$$n(t) = \int_0^{\infty} [\alpha_O C_O(x, t) + \alpha_R C_R(x, t)] \exp(-x/l) d(x/l) \quad (2)$$

When the measurement time is larger than the diffusion time of the reaction species over a distance of  $l \sim 100$  nm, we can simplify eq (2) as:

$$n(t) \approx \alpha_O C_O(x, t) + \alpha_R C_R(x, t) \quad (3)$$

where  $C_O(x, y, z, t)|_{z=0}$  and  $C_R(x, y, z, t)|_{z=0}$  are the oxidized and reduced molecule concentrations near the electrode. In dilute solutions, the diffusion coefficient range of most ions and molecules is from  $10^{-9}$  to  $10^{-11}$  m<sup>2</sup>/s [16]. For most electrochemical reactions, the measurement time is at the order of 1 to  $10^3$  s, which gives rise to the diffusion distance around  $(2Dt)^{1/2} \approx 10^{-6}$  to  $10^{-3}$  m. Eq (3) is applicable. Furthermore, Eq (3) implies that local complex refractive index is the linear function of the concentration of oxidized and reduced species on the electrode surface.

For a typical redox reaction



the concentration of the oxidized and the reduced molecules are described by Fick's second law [17]:

$$\frac{\partial C}{\partial t} = D \frac{\partial^2 C}{\partial x^2} \quad (4)$$

where  $C(x, t)$  and  $D$  are the concentration and the diffusion coefficient. For a given system, the initial and the boundary conditions will give us a definite solution.

For diffusion-controlled electrochemical reactions, one of the boundary conditions is given by [18]

$$j = NFD_O \frac{\partial C_O}{\partial z} \Big|_{z=0} = -NFD_R \frac{\partial C_R}{\partial z} \Big|_{z=0} \quad (5)$$

where  $j$  is the current density versus potential or time, which is also a function of  $C_O$  and  $C_R$ ,  $N$  is the number of electrons transferred

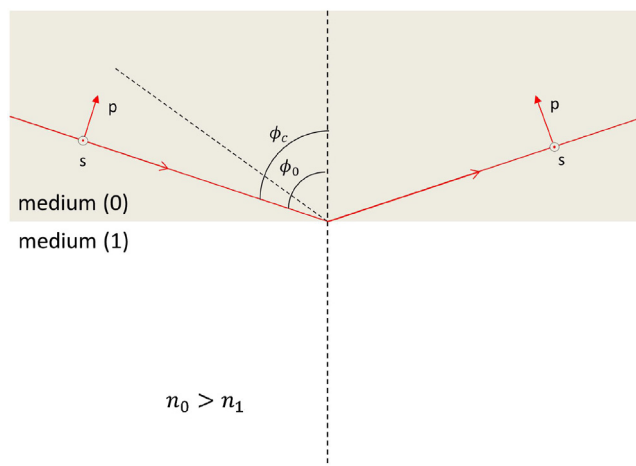


Fig. 1. Total internal reflection at a dielectric interface:  $\phi_c$ , angle of incidence over which the total internal reflection occurs;  $n_0$ ,  $n_1$ , refractive indices of the media.

per reaction,  $F$  is Faraday constant, and  $D_O$  and  $D_R$  are the diffusion coefficients of the reaction species. Comparing eqs (3) and (5), we can see that both local complex index of refraction and current are the functions of the reactant and product concentrations near the electrode. Where the refractive index measures the concentration in the vicinity of the working electrode surface, the current measures the local concentration gradient.

To demonstrate further relationship between TIRE signal and the redox-induced refractive index change near the electrode, a quantitative calculation should be established.

Considering the total internal reflection at a dielectric interface in Figure 1, we have [19]

$$|r_p| = |r_s| = 1 \quad (6)$$

$$\Psi = 45^\circ \quad (7)$$

$$\Delta = 2 \arctan \frac{(\sin^2 \phi_0 - \sin^2 \phi_c)^{1/2}}{\sin \phi_0 \tan \phi_0} \quad (8)$$

When redox reactions occur at the electrode, the local complex index of refraction  $n$  varies due to the change of  $C_O$  and  $C_R$ . For dilute solutions, we could assume the variation of the local refractive index  $\delta n$  is subtle [20]. Thus, the local complex index of refraction is given by

$$n(t) = n_1 + \delta n(t) \quad (9)$$

when  $t = 0$ ,  $n(0) = n_1$ .

The critical angle  $\phi_c$  is a function of the local refractive index  $n$  and the relationship is given by

$$\sin \phi_c = \frac{n}{n_0} \quad (10)$$

Eq (10) indicates that not only will the redox reactions on the surface of the electrode change the local complex index of refraction  $n$ , but also modulate the critical angle  $\phi_c$ . Substituting  $\sin \phi_c$  in eq (8), we get

$$\Delta(t) = 2 \arctan \frac{[\sin^2 \phi_0 - \frac{n(t)^2}{n_0^2}]^{1/2}}{\sin \phi_0 \tan \phi_0} \quad (11)$$

Expanding  $\Delta$  by Taylor expansion, we have

$$\delta \Delta \approx \frac{2n_1 n_0 \sin^2 \phi_0 \cos \phi_0}{\sqrt{n_0^2 \sin^2 \phi_0 - n_1^2 (n_1^2 \cos^2 \phi_0 - n_0^2 \sin^2 \phi_0)}} \delta n \quad (12)$$

Or more simply,

$$\delta\Delta \propto \delta n \quad (13)$$

Since TIRE enjoys the interface and thin-film sensitivity in  $\Delta$  for angles larger than the critical angle [19], we can use TIRE technique to detect the redox-induced variation of the local complex refractive index.

For a conventional polarizer-compensator-sample-analyzer (PCSA) ellipsometric system, the detected intensity of the polarized light is given by [21]

$$I = \frac{1}{2} K |r_s|^2 \{ [1 + \cos 2\hat{C} \cos 2(P - \hat{C})] \cos^2 A \tan^2 \Psi + [1 - \cos 2\hat{C} \cos 2(P - \hat{C})] \sin^2 A + [\sin 2\hat{C} \cos 2(P - \hat{C}) \cos \Delta - \sin 2(P - \hat{C}) \sin \Delta] \sin 2A \tan \Psi \} \quad (14)$$

where  $P$ ,  $\hat{C}$ ,  $A$  are the azimuth angles of the polarizer, the compensator, and the analyzer respectively.  $K$  is the sensitivity constant determined by the given TIRE setup.

To detect the redox-induced local complex refractive index variation on the electrode surface, the PCSA ellipsometric system works under the null and off-null mode: it fulfills the null condition when no redox reaction occurs and applies the off-null condition when the redox reaction happens. By Taylor expansion and eqs (6) and (7), the variation of the intensity of the polarized light caused by the reaction is given by

$$\delta I = -\frac{1}{2} \kappa \sin 2A [\sin 2\hat{C} \cos 2(P - \hat{C}) \sin \Delta + \sin 2(P - \hat{C}) \cos \Delta] \delta \Delta \quad (15)$$

Or

$$\delta I \propto \delta \Delta \quad (16)$$

By eqs (13) and (16), we have

$$\delta I \propto \delta n \quad (17)$$

## 2.2. Chemicals

Sodium chloride (KCl) is purchased from Sigma-Aldrich and sodium hydroxide (NaOH) and pure ethanol from Beijing Chemical Works. All the compounds used in this work are in analytical grade without further purification. Ultrapure water is obtained from a MILLI-Q purification system (18.2 M $\Omega$  at the room temperature) and used to prepare all the solutions.

To detect the reduction of DO on the gold surface, 0.1 M NaCl electrolyte is prepared. To avoid the interference of protons, 1 mM NaOH is added. Different DO concentration samples are obtained by bubbling mixed oxygen and nitrogen.

## 2.3. Instrumentation

The Electrochemical experiments are performed using a VersaSTAT 3 electrochemical system (Princeton, U.S.A). To observe the reaction-induced refractive index change on the gold electrode, a 29 mm  $\times$  17 mm SF10 glass slide covered with a 2-nm-thick Cr adhesive under-layer and a 50-nm-thick gold film serves as both the sensing surface and the cathode of the electrode, a silver/silver chloride (Ag/AgCl) electrode as the reference and a Pt wire electrode as the counter. Prior to each experiment, the gold film is cleaned with the ultrapure water and pure ethanol to remove the possible surface contamination and then blown to dry.

Figure 2 illustrates the EC-TIRE setup used for all experiments described in this paper. A SF10 trapezoidal prism is used with a Xe lamp as the light source and a high-speed CCD camera as the

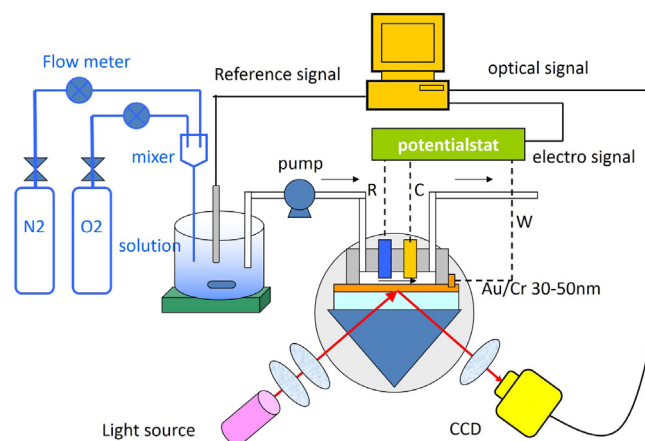


**Fig. 2.** Schematic illustration of EC-TIRE system. The nitrogen is bubbled into the electrolyte to eliminate the oxygen and then the electrolyte is pumped into the experimental cell. The redox reaction in the experimental cell is measured by both an optical system and an electrical system. An external electrochemistry station is applied for the electrochemical condition. Both the optical and electrical signals are recorded by a computer.

detector. The 632.8 nm light beam is guided by an optical fiber and expanded by a collimating system. After passing a polarizer and a compensator, the polarized collimated beam propagates perpendicularly to the prism and onto the sensing surface. When the incident angle is optimized as 65°, larger than the critical angle, the evanescent wave appears sharply at the sensing surface to detect the interaction in very shallow depth from the surface. The reflected light carrying the surface information is then imaged by a CCD camera after passing an analyzer. The system works under the null and off-null mode, which almost fulfills the null condition on the bare gold when no redox reactions occur and detects the refractive index change under the off-null condition. Combined with an external electrochemical working station, this configuration allows for simultaneously TIRE detection of the index variation of refraction on the gold surface and the electrochemical measurement. During the measurement, the complex refractive index change caused by the DO reduction is recorded by TIRE in grayscale.

Figure 3 depicts the electrochemical cell for Clark type electrode. The cell is divided into two compartments by an oxygen permeable membrane: a sample compartment and an electrolyte compartment. Samples with different DO concentrations are pumped into the sample compartment. The DO in the sample diffuses into the electrolyte through the gas-permeable membrane and is reduced on the gold surface when a polarized potential  $-800$  mV (vs. Ag/AgCl)

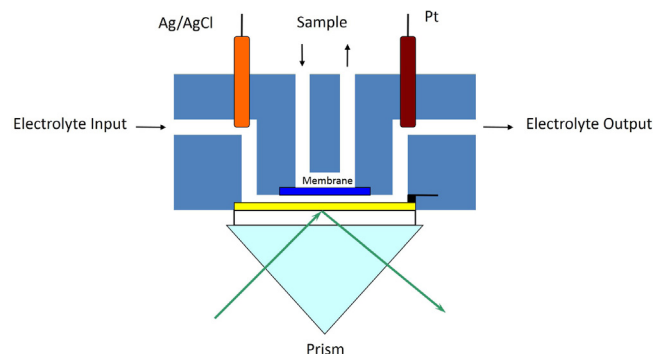
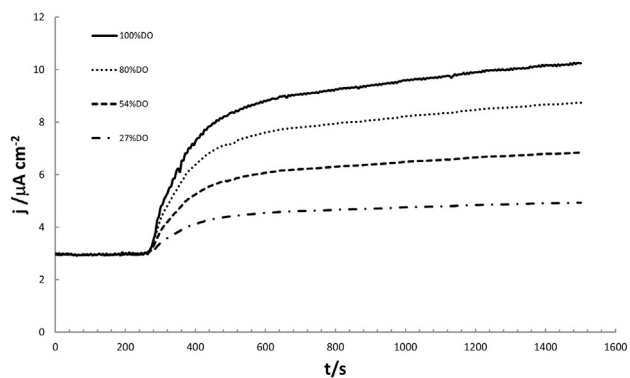
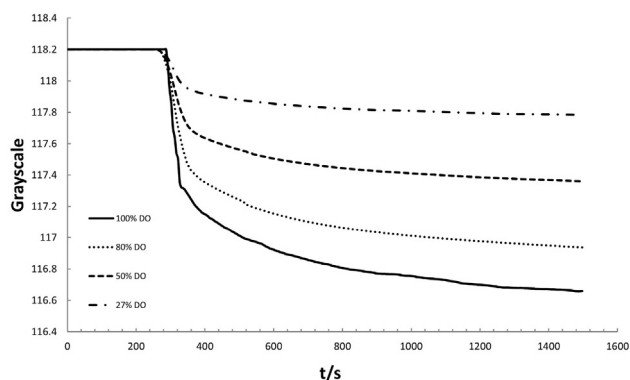


**Fig. 3.** The experimental cell for DO reduction. An oxygen permeable membrane is put on the top of the gold electrode, separating the cell into a sample compartment and an electrolyte compartment. DO in the sample compartment will diffuse through the membrane into the electrolyte, 0.1 M NaCl with 1 mM NaOH. When a polarized potential is applied, DO is reduced at the gold surface.



(a) The current density change for different DO concentrations.



(b) The TIRE signal change (grayscale) for different DO concentrations.

**Fig. 4.** 4(a) The current density change for different DO concentrations. The initial current density indicates a sample without DO. During 300 s, the samples with different DO concentrations have been pumped into the cell, which will increase the current density. 4(b) TIRE signal change for different DO concentrations. The change synchronizes with the current density variation, which indicates that EC-TIRE is capable of detecting DO reduction on the gold surface.

is applied. The distance between the gold sensing surface and the membrane is about 1 mm.

### 3. Results and Discussion

Figure 4 shows that the real time EC-TIRE curves for different DO concentrations. When the samples with DO have been delivered into the cell, DO is reduced at the electrode. Thus, the current changes. The TIRE signal varies synchronously. When the redox reaches equilibrium, both electric signal and TIRE signal flaten.

#### 3.1. Semi-infinite Boundary Condition vs. Finite Boundary Condition

S. Wang, X. Huang, X. Shan, K.J. Foley and N. Tao have developed an analytical solution for SPR signal under one-dimensional and semi-infinite conditions [15]. The solution is applicable when the size of the cell is much larger than the diffusion distance during the measurement time. By the similar procedure, we have:

$$\delta C_O = -D_O^{-1/2}(NF\pi^{1/2})^{-1} \int_0^t j(\tau)(t-\tau)^{-1/2} d\tau \quad (18)$$

$$\delta n = (\alpha_R D_R^{-1/2} - \alpha_O D_O^{-1/2})(NF\pi^{1/2})^{-1} \int_0^t j(\tau)(t-\tau)^{-1/2} d\tau \quad (19)$$

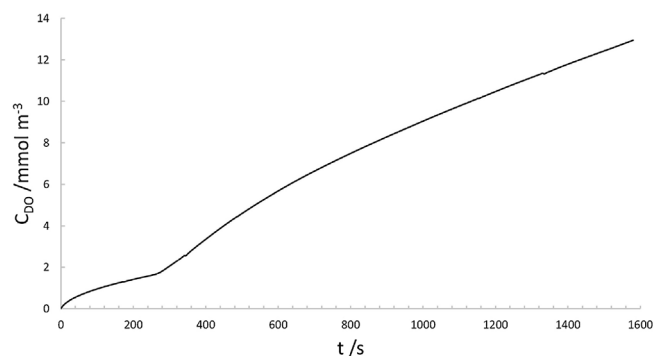


**Fig. 5.** DO concentration at the surface of the electrode calculated from the measured current density of 100% DO concentration sample. The calculation is based on the semi-infinite condition.

For a specific reaction,  $\alpha_R$ ,  $\alpha_O$ ,  $D_R$ ,  $D_O$ ,  $n$ ,  $F$  are constants, so we have

$$\delta n \propto \delta C_O \quad (20)$$

By eqs (17) and (20), we can expect that the TIRE signal under the semi-infinite condition should be proportional to the local reactant concentration. Taking the current density as input, we have calculated the DO concentration by eq (18) in Figure 5. Both the steady state and the dynamic process are considered. It can be seen that the calculated DO concentration from the current does not agree with the experimental data at all. The reason is that when the size of the cell is comparable to the diffusion distance, the semi-infinite condition would fail. For conventional Clark electrode, an oxygen permeable membrane is usually on the top of the working electrode [22]. The distance between the membrane and the electrode is at the order of  $10^{-3}$  m. Since the measurement time is at the order of  $10^2$  to  $10^3$  s, the diffusion distance is around  $(2D_{DO}t)^{1/2} \approx 10^{-3}$  m. Therefore, a solution based on the finite geometry needs to be proposed.

#### 3.2. Steady State Measurement

Let us consider the one-dimension (along  $x$ -axis) diffusion. During the steady state measurement, the concentration is only the function of the diffusion distance  $x$ . Thus, eq (4) degrades to an ordinary differential equation:

$$\frac{d^2 C_{DO}}{dx^2} = 0 \quad (21)$$

The boundary conditions are given by:

$$j = NFD_{DO} \frac{dC_{DO}}{dx} \Big|_{x=0}, \text{ at the electrode surface, where } x = 0 \quad (22)$$

$$C_{DO}(l) = C^0, \text{ at the membrane surface, where } x = l \quad (23)$$

where  $C^0$  is the DO concentration in the sample solution.

By considering the boundary conditions (22) and (23), the solution to eq (21) is

$$C_{DO}(x) = \frac{jx}{NFD_{DO}} + \left( C^0 - \frac{j l}{NFD_{DO}} \right) \quad (24)$$

Thus, the DO concentration at the electrode surface ( $x=0$ ) is given by

$$C_{DO}(0) = C^0 - \frac{j l}{NFD_{DO}} \quad (25)$$

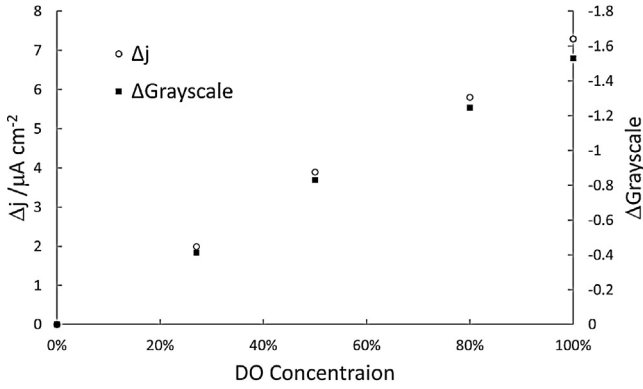


**Fig. 6.** As predicted by eq (29), when the measurement approaches steady, both electric signal change and TIRE signal change should be proportional to the DO concentration.

The electrolyte for Clark electrode is usually added with the excessive alkali solution [10], which indicates that the hydroxyl ions reduced from the oxygen is far less than the bulk hydroxyl concentration  $C^*$ . Therefore, the boundary condition at the membrane is given by

$$C_{OH}(l) = C^* \quad (26)$$

Using the similar procedure for  $C_{DO}$ , we can get

$$C_{OH}(0) = C^* + \frac{jI}{NFD_{OH}} \quad (27)$$

Combining eqs (3), (9), (25) and (27), we have

$$\delta n = \left( \frac{\alpha_{OH}l}{NFD_{OH}} - \frac{\alpha_{DO}l}{NFD_{DO}} \right) \delta j \quad (28)$$

By eq (17), the relationship between the current density and the TIRE signals under the steady state measurement is given by

$$\delta I = M\delta j \quad (29)$$

where  $M$  is the sensitivity constant determined by TIRE setup and the reaction species.

Eq (29) suggests that TIRE signal would be a linear function of the current density during the steady state measurement. As is shown in Figure 6, not only the current density change is proportional to the oxygen concentration in the sample ( $y = 7.2682x + 0.0631$ ,  $R^2 = 0.9958$ ), but the TIRE signal variation ( $y = -1.5386x - 0.0132$ ,  $R^2 = 0.9979$ ). The results prove that TIRE have the potential to be used as DO probe for steady state measurement.

### 3.3. Dynamic Measurement

During this measurement condition, the diffusion equation of the oxygen is

$$\frac{\partial C_{DO}}{\partial t} = D_{DO} \frac{\partial^2 C_{DO}}{\partial x^2} \quad (30)$$

where  $C_{DO}(x, t)$  and  $D_{DO}$  are the concentration and diffusion coefficient of DO.

To simplify the question, we assume that at the beginning, there is no oxygen in the electrolyte, that is

$$C_{DO}(x, 0) = 0, \quad 0 \leq x \leq l \quad (31)$$

Thus, we have (see the appendix for the deduction)

$$\begin{aligned} C_{DO}(0, t) = & 2C^0 \sum_{n=0}^{\infty} (-1)^n \operatorname{erfc} \left[ (D_{DO}t)^{-1/2} \frac{(2n+1)l}{2} \right] \\ & - \frac{1}{NF} \sum_{n=0}^{\infty} (-1)^n \int_0^t \frac{j(\tau)}{\sqrt{D_{DO}\pi(t-\tau)}} \exp \left[ -\frac{n^2l^2}{D_{DO}(t-\tau)} \right] d\tau \\ & + \frac{1}{NF} \sum_{n=0}^{\infty} (-1)^n \int_0^t \frac{j(\tau)}{\sqrt{D_{DO}\pi(t-\tau)}} \exp \left[ -\frac{(n+1)^2l^2}{D_{DO}(t-\tau)} \right] d\tau \end{aligned} \quad (32)$$

By assuming the amount of hydrogen peroxide is so small that we do not consider its influence, similarly, we can get the concentration for the reduced species, the hydroxyl ions, which is given by

$$\begin{aligned} C_{OH}(0, t) = & 2C^* \sum_{n=0}^{\infty} (-1)^n \operatorname{erfc} \left[ (D_{OH}t)^{-1/2} \frac{(2n+1)l}{2} \right] \\ & + \frac{1}{NF} \sum_{n=0}^{\infty} (-1)^n \int_0^t \frac{j(\tau)}{\sqrt{D_{OH}\pi(t-\tau)}} \exp \left[ -\frac{n^2l^2}{D_{OH}(t-\tau)} \right] \\ & \times d\tau - \frac{1}{NF} \sum_{n=0}^{\infty} (-1)^n \int_0^t \frac{j(\tau)}{\sqrt{D_{OH}\pi(t-\tau)}} \\ & \exp \left[ -\frac{(n+1)^2l^2}{D_{OH}(t-\tau)} \right] d\tau \end{aligned} \quad (33)$$

Since we assume the initial concentrations for  $C_{DO}$  and  $C_{OH}$  are 0 at the electrode surface, according to eqs (3) and (17), we have

$$\delta I = M\delta n = M[\alpha_{DO}C_{DO}(0, t) + \alpha_{OH}C_{OH}(0, t)] \quad (34)$$

where  $M$  is the sensitivity constant determined by TIRE setup and the reaction species.

### 3.4. Membrane Diffusion Influence

During the dynamic measurement, we assume when a step concentration is applied to the sample, the concentration in the electrolyte at the membrane would reach equilibrium with the sample concentration  $C^0$  instantaneously. However, because it takes time for DO in the sample to diffuse through the membrane, it would be more reasonable to assume the concentration at the membrane surface is initially zero and approaches an equilibrium concentration  $C^0$  exponentially [23], i.e.,

$$C_{DO}(l, t) = C^0[1 - \exp(-t/\tau_p)] \quad (35)$$

where  $\tau_p$  is the sensor time constant, when the sensor response reaches 63.7% of its ultimate response. Thus, the DO concentration during the dynamic measurement should be added with a membrane correction term  $C_m$ , i.e.,

$$\begin{aligned} C_m = & -C^0 \sum_{n=0}^{\infty} (-1)^n \int_0^t \frac{(2n+1)l}{\sqrt{\pi D_{DO}(t-\tau)^3}} \\ & \exp \left[ -\frac{(2n+1)^2l^2}{4D_{DO}(t-\tau)} - \frac{t}{\tau_p} \right] d\tau \end{aligned} \quad (36)$$

Figure 7 has demonstrated that during the dynamic measurement, the calculated dynamic curve without the consideration of the membrane diffusion influence ( $\alpha_{DO}M = -0.2551$  grayscale/M,

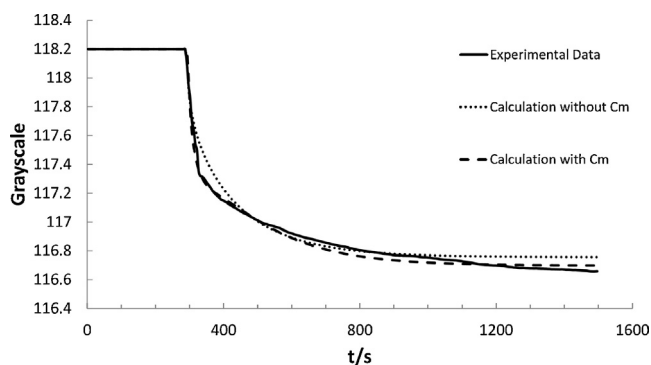


**Fig. 7.** The theoretical calculations of the measurement of 100% concentration DO. For the steady-state measurement, the stable current density suggests TIRE signal should be a straight line, as predicted by eq (29). For the dynamic measurement, although both calculation curves are in agreement in shapes with the experimental data, the one with the consideration of membrane diffusion influence  $C_m$  is a better fitting.

$\alpha_{OH}M = -0.3071$  grayscale/M) is in good agreement with the experimental data in shape ( $R^2 = 0.9314$ ), but the experimental data takes more time to get stable. As we have mentioned, it is because when a step concentration is applied, the concentration in electrolyte at the membrane would exponentially approach to the equilibrium concentration  $C^0$ . When we take into account the membrane correction term  $C_m$  ( $\tau_p = 341$  s), the agreement between the theoretical calculation and the experimental data ( $\alpha_{DO}M = -0.5287$  grayscale/M,  $\alpha_{OH}M = -0.8434$  grayscale/M) has been improved ( $R^2 = 0.9631$ ), especially during the time 272 to 507 s when TIRE signal jumps. The difference between the later parts of the curves might owe to the hydrogen peroxide generated during the reduction. In spite of the difference, both the experimental data and the theoretical calculation suggest that when the current reaches 90% of its steady state current, TIRE signal reaches 92% of its steady state current. Thus, TIRE also has the potential to be used as the dynamic measurement.

Despite the small change of the optical signal, the synchronization of the optical and electrochemical signals indicates a new approach to analyze DO in the liquid and the possibility of using the TIRE technique to monitor the refractive index change in the neighborhood of the electrode surface.

#### 4. Conclusion

EC-TIRE has been introduced to observe the reaction-induced refractive change caused by the DO reduction at Clark electrode. Compared with the semi-infinite boundary condition, a thin layer model has been established for both the steady state measurement and the dynamic measurement. By considering the membrane diffusion influence, the theoretical calculation is in good agreement with the experimental data in both shape and values. The results demonstrated that EC-TIRE have the potential to monitor DO concentration.

For the diffusion-controlled electrochemical reactions, a small ratio of electrode area,  $A$ , to solution volume,  $V$  allows the experiments to be carried out over long time without significant change of the electroactive species in the bulk solution. Thus, a semi-boundary condition is applicable for the refractive index change. However, in a number of analytical measurements, the large  $A/V$  allows electroactive species exhaustion. The thin layer model could be more suitable to describe the refractive index change.

By introducing an imaging technique, a potential for quick dissolve oxygen detection can be foreseen. More specifically, during the practical measurement, the drift of the electrical signal can restrict the accuracy of the measurement. To overcome this

disadvantage, a real-time DO measurement by a synchronized electrochemical and optical approach will be proposed. When drift occurs, the optical signal can tell whether the change of the electrical signal is caused by different DO concentration or other factors.

#### Acknowledgement

The authors acknowledge the financial support to the National Natural Science Foundation of China (21305147), to the International Science & Technology Cooperation Program of China (2012DFG31880), to the National Basic Research Program of China (2009CB320302), to the National High Technology Research Development Program of China (2008AA02Z419), and to the Instrument Developing Project of the Chinese Academy of Sciences (KJXC2-YW-M04, KJXC2-YW-M03).

#### Appendix A. DO Concentration during the Dynamic Process

Performing Laplace transform on eq (30), we have

$$p\tilde{C}_{DO}(x, p) = D_{DO} \frac{\partial^2 \tilde{C}_{DO}(x, p)}{\partial x^2} \quad (37)$$

where  $\tilde{C}_{DO}(x, p)$  is the Laplace transform of  $C_{DO}(x, t)$ . The solution of eq (37) is

$$\tilde{C}_{DO}(x, p) = A(p) \exp(-qx) + B(p) \exp(qx) \quad (38)$$

where  $q^2 = p/D_{DO}$ ,  $A(p)$  and  $B(p)$  are functions to be determined by the boundary conditions.

At the electrode surface, where  $x=0$ , the oxygen concentration satisfies eq (5). By using Laplace transform to eq (5), we have

$$\tilde{j}(p) = nFD_{DO} \frac{\partial \tilde{C}_{DO}}{\partial x} \Big|_{x=0} \quad (39)$$

At the membrane, where  $x=l$ , the oxygen concentration reaches equilibrium with that in the sample solution  $C^0$ ,

$$C_{DO}(l, t) = C^0 \quad (40)$$

The Laplace transform of eq (40) is given by

$$\tilde{C}_{DO}(l, p) = \frac{C^0}{p} \quad (41)$$

Thus, by the boundary conditions (39) and (41) and eq (38), we have

$$\tilde{C}_{DO}(0, p) = \frac{1}{q \cosh(ql)} \left[ \frac{q}{p} C^0 - \frac{\sinh(ql)}{NFD_{DO}} \tilde{j}(p) \right] \quad (42)$$

We express eq (42) in terms of negative potentials and expand in a series by binomial theorem

$$\begin{aligned} \tilde{C}_{DO}(0, p) &= \frac{2C^0}{p} \frac{\exp(-ql)}{1 + \exp(-2ql)} - \frac{\tilde{j}(p)}{NFD_{DO}} \frac{1 - \exp(-2ql)}{1 + \exp(-2ql)} \\ &= \frac{2C^0}{p} \exp(-ql) \sum_{n=0}^{\infty} (-1)^n \exp(-2nql) - \frac{\tilde{j}(p)}{NFD_{DO}} \sum_{n=0}^{\infty} (-1)^n \\ &\quad \exp(-2nql) + \frac{\tilde{j}(p)}{NFD_{DO}} \exp(-2ql) \sum_{n=0}^{\infty} (-1)^n \exp(-2nql) \end{aligned} \quad (43)$$

Using inverse Laplace transform and convolution theorem, we will have eq (32).

By the similar procedure, we can have eqs. (33) and (26).

## References

- [1] M. Poksinski, H. Dzuho, H. Arwin, Copper corrosion monitoring with total internal reflection ellipsometry, *Journal of the Electrochemical Society* 150 (11) (2003) B536–B539.
- [2] M. Poksinski, H. Arwin, In situ monitoring of metal surfaces exposed to milk using total internal reflection ellipsometry, *Sensors and Actuators B: Chemical* 94 (3) (2003) 247–252.
- [3] M. Poksinski, H. Arwin, Protein monolayers monitored by internal reflection ellipsometry, *THIN SOLID FILMS* 455 (2004) 716–721, 3rd International Conference on Spectroscopic Ellipsometry (ICSE-3), Vienna, AUSTRIA, JUL 06-12, 2003.
- [4] L. Novotny, B. Hecht, *Principles of nano-optics*, Cambridge university press, 2012.
- [5] L. Liu, Y. Niu, S. Chen, Y. Meng, H. Ma, G. Jin, Optimization of evanescent wave imaging for the visualization of protein adsorption layers, *Science China Physics, Mechanics and Astronomy* 53 (10) (2010) 1805–1810.
- [6] L. Liu, Y. Niu, Y.H. Meng, S. Chen, X.Y. Yan, G. Jin, CD146 detection with real-time total internal reflection imaging ellipsometry, in: Vol. 25 of IFMBE Proceedings, Springer, New York, 2009, pp. 34–36.
- [7] C.O. Moses, D. Kirk Nordstrom, J.S. Herman, A.L. Mills, Aqueous pyrite oxidation by dissolved oxygen and by ferric iron, *Geochimica et Cosmochimica Acta* 51 (6) (1987) 1561–1571.
- [8] L.H. Gray, A. Conger, M. Ebert, S. Hornsey, O. Scott, The concentration of oxygen dissolved in tissues at the time of irradiation as a factor in radiotherapy, *British Journal of Radiology* 26 (312) (1953) 638–648.
- [9] K. Kaiho, Benthic foraminiferal dissolved-oxygen index and dissolved-oxygen levels in the modern ocean, *Geology* 22 (8) (1994) 719–722.
- [10] Y.H. Lee, G.T. Tsao, *Dissolved oxygen electrodes*, Springer, 1979.
- [11] M. Forbes, S. Lynn, Oxygen reduction at an anodically activated platinum rotating disk electrode, *AIChE Journal* 21 (4) (1975) 763–769.
- [12] B. Bandyopadhyay, A. Humphrey, H. Taguchi, Dynamic measurement of the volumetric oxygen transfer coefficient in fermentation systems, *Biotechnology and Bioengineering* 9 (4) (1967) 533–544.
- [13] A.A. Benedek, W.J. Heideger, Polarographic oxygen analyzer response: The effect of instrument lag in the non-steady state reaeration test, *Water Research* 4 (9) (1970) 627–640.
- [14] I.J. Dunn, A. Einsele, Oxygen transfer coefficients by the dynamic method, *Journal of Applied Chemistry and Biotechnology* 25 (9) (1975) 707–720.
- [15] S. Wang, X. Huang, X. Shan, K.J. Foley, N. Tao, Electrochemical surface plasmon resonance: basic formalism and experimental validation, *Anal Chem* 82 (3) (2010) 935–941.
- [16] C. Wilke, P. Chang, Correlation of diffusion coefficients in dilute solutions, *AIChE Journal* 1 (2) (1955) 264–270.
- [17] C. J., *The Mathematics of Diffusion*, Elsevier, 1975.
- [18] A.J. Bard, L.R. Faulkner, *Electrochemical Methods: Fundamentals and Applications*, 2nd Edition, Wiley, 2000.
- [19] H. Arwin, M. Poksinski, K. Johansen, Total internal reflection ellipsometry: principles and applications, *Applied optics* 43 (15) (2004) 3028–3036.
- [20] A. Wolf, V. Pillay, Renal concentration tests: Osmotic pressure, specific gravity, refraction and electrical conductivity compared, *The American journal of medicine* 46 (6) (1969) 837–843.
- [21] Y. Chen, Y. Meng, G. Jin, Optimization of off-null ellipsometry for air/solid interfaces, *Applied optics* 46 (35) (2007) 8475–8481.
- [22] L.C. Clark, R. Wolf, D. Granger, Z. Taylor, Continuous recording of blood oxygen tensions by polarography, *Journal of Applied Physiology* 6 (3) (1953) 189–193.
- [23] J. Mueller, W. Boyle, E. Lightfoot, Effect of the response time of a dissolved oxygen probe on the oxygen uptake rate, *Applied microbiology* 15 (3) (1967) 674.